

Ordered 180° ferroelectric domains in epitaxial submicron structures

Ionela Vrejoiu,^{a)} Alessio Morelli, Florian Johann, and Daniel Biggemann
 Max Planck Institute of Microstructure Physics, Weinberg 2, 06120 Halle Germany

(Received 20 June 2011; accepted 9 August 2011; published online 25 August 2011)

Large range ordered $\text{La}_{0.7}\text{Sr}_{0.3}\text{MnO}_3$ and SrRuO_3 epitaxial dots were fabricated by pulsed laser deposition using stencil masks and were embedded in ferroelectric PbTiO_3 epitaxial films. PbTiO_3 films grown on top of $\text{La}_{0.7}\text{Sr}_{0.3}\text{MnO}_3$ dots form arrays of 180° domains that are switchable and have good ferroelectric properties. PbTiO_3 films made on top of SrRuO_3 dots have a monodomain polarization state. These observations point out the importance of the electronic properties of the bottom electrode in the selection of a preferential polarization state in epitaxial ferroelectric films and propose a route of fabricating large arrays of switchable 180° ferroelectric domains. © 2011 American Institute of Physics. [doi:10.1063/1.3630232]

The demands for miniaturization of functional oxides require elaborate methods of top-down patterning and bottom-up synthesis of nanostructures, involving many and often very laborious processing steps. Additionally, the effects of decreasing the size on the physical properties of the structures have to be investigated and well understood. Among functional oxides, ferroelectric, ferromagnetic, and ferrimagnetic oxides and their combination in hybrid multiferroic structures, with various possible mechanisms of magnetoelectric coupling, have been fabricated by various techniques and their physical properties are under intensive study.^{1–6} Ferroelectric $\text{Pb}(\text{Zr},\text{Ti})\text{O}_3$ nanocapacitors were fabricated in densities as high as 176 Gbit/in², approaching densities interesting for nonvolatile data-storage applications.⁷

We report on the fabrication of arrays of epitaxial $\text{La}_{0.7}\text{Sr}_{0.3}\text{MnO}_3$ (LSMO) and SrRuO_3 (SRO) submicron sized-dots, with large range order, which are embedded in epitaxial ferroelectric PbTiO_3 (PTO) films. The polarization of the tetragonal *c*-axis ferroelectric PTO film as-grown on top of LSMO dots shows either upwards or downwards orientations, depending on the electronic properties of the bottom interface. Hence, arrays of well ordered and switchable 180° ferroelectric domains can be directly fabricated.⁸ In the case of the PTO film grown on top of SRO dots, the polarization is oriented uniformly downwards, most probably due to uniform metallic properties of the bottom interface of the ferroelectric film.

The epitaxial heterostructures were fabricated by pulsed-laser deposition. Semiconductive Nb-doped SrTiO_3 (100)-oriented crystals were used as substrates. For the growth of the LSMO and SRO dots, stencil masks were applied on the substrates. The stencils consisted of amorphous SiN membranes on Si wafers, with arrays of hexagonally ordered circular apertures of 800 nm diameter.^{9,10} The epitaxial dotlike structures were grown *in situ* with the stencil attached mechanically to the substrates, at temperatures of about 600 °C, in oxygen pressures of 2.7×10^{-2} mbar. After removing the stencil mask, the substrate with the LSMO or SRO dots was reheated to 585 °C and a PbTiO_3 film was deposited in 0.25 mbar O₂.

The topography and the ferroelectric properties of the PTO/LSMO and PTO/SRO heterostructures were probed by means of piezoresponse force microscopy (PFM) performed with two different commercial atomic force microscopes, a MFP-3D Asylum Research with an external lock-in amplifier (SRS830 DSP Stanford Research Systems) and a XE-100 Park System. Cross section specimens for transmission electron microscopy were prepared by focused ion beam (FEI Nova NanoLab 600) milling of thin lamellae. High angle annular dark field scanning transmission electron microscopy (HAADF-STEM) and energy dispersive x-ray spectroscopy (EDX) were performed in a FEI Titan 80-300 microscope with a spherical aberration corrected probe forming system.¹¹

Piezoresponse force microscopy investigations of an epitaxial PTO film (50 nm thick), on top and in between the LSMO dots (~27 nm thick, deposited through stencil with 800 nm diameter apertures), revealed a surprising behavior of the orientation of the PTO polarization. Figure 1(a) shows a topography image (5 μm × 5 μm large area) and Fig. 1(b) the corresponding out-of-plane PFM phase image in which the bright contrast corresponds to upwards polarization and the dark contrast to downwards polarization. In between the LSMO dots, where the tetragonal PTO film grows *c*-axis oriented on the Nb-STO substrate, the polarization is uniformly pointing upwards. Directly on top of the LSMO dot and partly on their wedgelike edges, the polarization is oriented upwards as well. However, around the LSMO dots, in regions of 50–200 nm width, the polarization of the PTO film turns to downwards orientation, as seen better in the out-of-plane PFM phase image shown in Fig. 1(d), corresponding to the area whose topography is imaged in Fig. 1(c). As indicated in Fig. 1(d), in the central part of the PTO film on top of the LSMO dot (500 nm × 500 nm area), a stable domain of downwards polarization was written by applying a bias voltage of +8 V_{DC} to the tip while scanning. Similarly, the nearby domain with as-grown downwards polarization was switched to upwards polarization by applying a bias voltage of –6 V_{DC}. Piezoresponse hysteresis loops of the PTO film measured on top of the LSMO dot (Fig. 1(e)) and in an area with downwards polarization, around the dot (Fig. 1(f)), showed similar piezoelectric responses, with slightly larger coercive voltage for the latter.

^{a)} Author to whom correspondence should be addressed. Electronic mail: vrejoiu@mpi-halle.de.

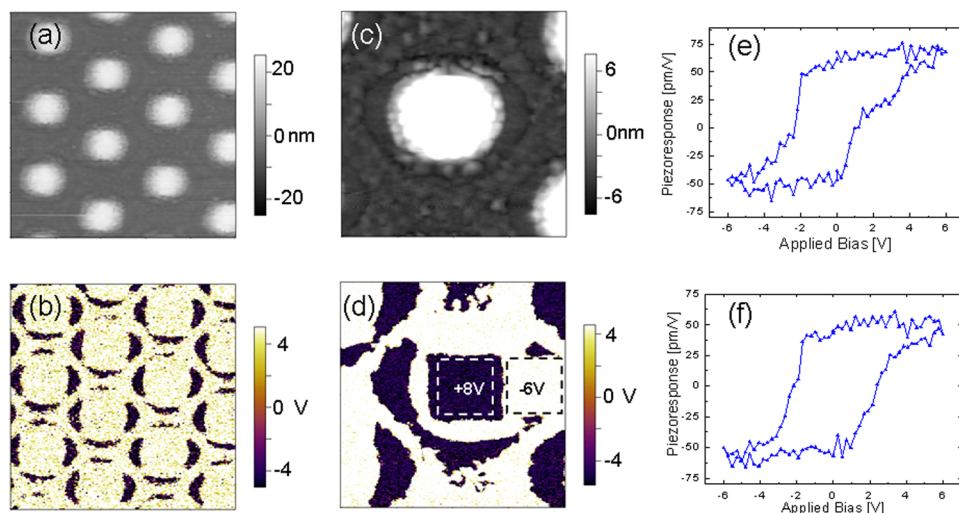


FIG. 1. (Color online) Piezoresponse force microscopy of the PTO film grown on top of LSMO dots on Nb-doped SrTiO₃(100): (a) topography image (5 μm × 5 μm) and (b) its corresponding out-of-plane PFM phase image. A topography image of a single dot structure (2 μm × 2 μm) is shown in (c) and its corresponding out-of-plane PFM phase image in (d). Piezoresponse hysteresis loops of the PTO film measured in the middle of a dot structure and in an area around the dot (with as-grown opposite polarization state) are shown in (e) and (f), respectively.

From the microstructure point of view, the regions where the polarization orientation changes 180° correspond to areas around the LSMO dots where the LSMO becomes few unit cells thick, as we observed by HAADF-STEM, which has atomic number Z-contrast and thus allows to have a closer look at the interfaces. The LSMO dots made through the circular apertures of the stencil have somewhat larger diameter than the stencil apertures and trunk-conical shape due to broadening effects and clogging of the stencil pores.⁹ Figure 2 shows two cross section HAADF-STEM micrographs taken close to the edge of the LSMO dot, as marked in the scheme shown as an inset in Fig. 2(a). Fig 2(b) shows the very end of the LSMO dot, where the thickness of LSMO gradually decreases from about five to one unit cells. Scanning further away from this dot edge (ca. 200 nm), we observed a direct interface between the PTO film and the Nb-doped STO substrate, where no Mn signal was detected by EDX line scans (not shown here) across the interface.

The change of the orientation of the polarization may be related to the change of the electronic properties and charge carrier densities of the LSMO when it becomes few unit cells thick. It was reported that LSMO epitaxial films grown on STO(100) become insulating and nonferromagnetic at a critical thickness of ~4 unit cells.¹² In order to check this hypothesis, we fabricated SRO dots (stencil with 800 nm diameter apertures) on Nb-doped STO(100), under the same conditions as for the fabrication of the LSMO dots, and embedded them in a PTO film. SRO epitaxial films have much better metallic conductivity than half-metallic p-type conducting LSMO epitaxial films and, when grown on STO(100), remain metallic down to one unit cell thick.¹³ Hence, we expect that the SRO dots should have uniform electrical properties, no matter their topography and thickness. Figure 3 summarizes the PFM investigations of a PTO film grown on top of SRO dots, with a topography image (10 μm × 10 μm area) given in Fig 3(a) and the corresponding out-of-plane piezoresponse phase image given in Fig. 3(b). The PTO film had uniform polarization with upwards orientation both on top and in between the SRO dots, and no regions of downwards polarization were detected. Figure 3(c) is a zoom-in topography image (4 μm × 4 μm), and Fig. 3(d) is its corresponding out-of-plane PFM phase image,

in which two domains (500 nm × 500 nm) of downwards polarization (dark contrast) were written on top of a dot and in between dots by applying +8 V_{DC} to the tip, during scanning. Piezoresponse hysteresis loops measured on the PTO film on top of two SRO dots and in between the dots are

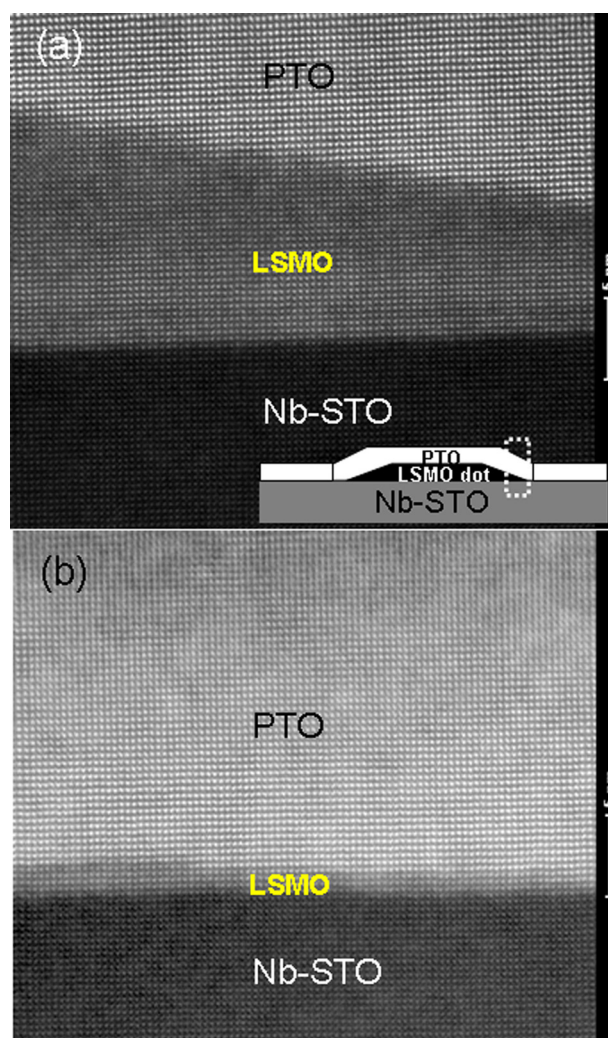


FIG. 2. (Color online) HAADF-STEM cross section micrographs taken at the edge of a PTO/LSMO dot structure, as indicated in the inset of (a). In (b), the very edge of the LSMO dot is imaged.

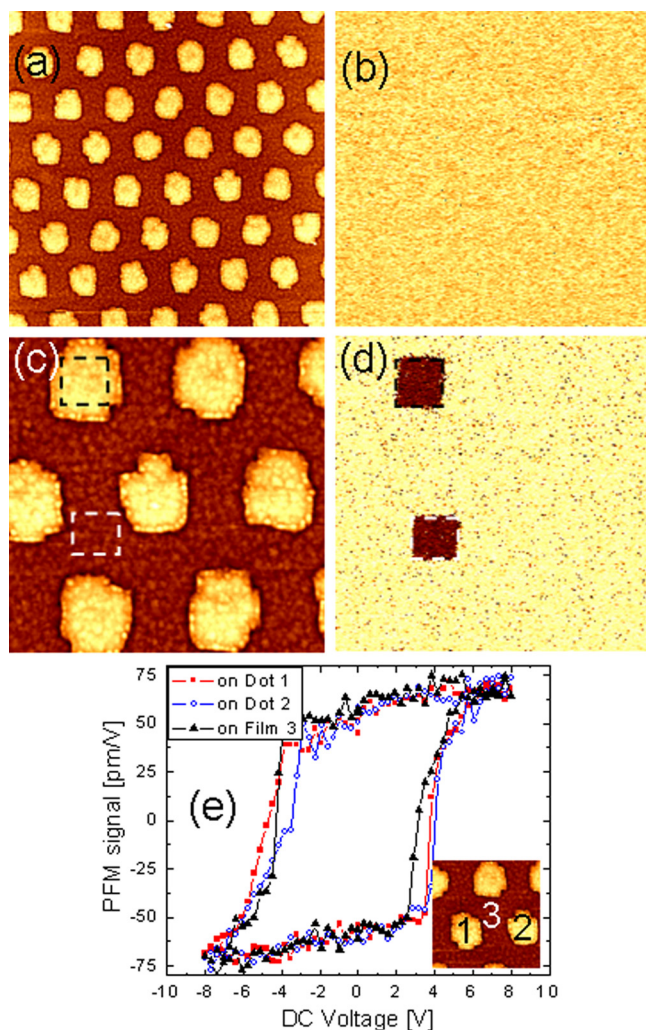


FIG. 3. (Color online) Piezoresponse force microscopy of the PTO film grown on top of SRO dots on Nb-doped $\text{SrTiO}_3(100)$: (a) topography image ($10 \mu\text{m} \times 10 \mu\text{m}$) and (b) its corresponding out-of-plane PFM phase image; (c) topography image ($4 \mu\text{m} \times 4 \mu\text{m}$) and (d) its corresponding out-of-plane PFM phase image in which two domains ($500 \text{ nm} \times 500 \text{ nm}$) of downwards polarization (dark contrast) were written on top of a dot and in between dots. (e) Piezoresponse hysteresis loops of the PTO film measured in the middle of two dot structures and in between dots (as indicated in the inset).

shown in Fig. 3(e) (as indicated in the topography image of the inset). No major differences could be observed between the hysteresis loops measured in these different areas of the PTO film.

The sudden transition from upwards to downwards polarization of the PTO film around the LSMO dots is intriguing. One may imagine subtle phenomena taking place in this region, such as a continuous 180° rotation of the electric dipoles, switching from upwards to downwards polarization, similar to what was recently imaged by aberration-corrected transmission electron microscopy, with atomic resolution, in epitaxial tetragonal c -axis oriented $\text{PbZr}_{0.2}\text{Ti}_{0.8}\text{O}_3$ films.¹⁴

It is also important to point out that our epitaxial PTO films grown on LSMO without breaking the vacuum have a preferential monodomain state, with polarization oriented

downwards, opposite to the case of the PTO film on top of LSMO dots. The former PTO films were fabricated by depositing first LSMO as a continuous bottom electrode at 650°C in 0.15 mbar O_2 on $\text{SrTiO}_3(100)$ substrates and then the PTO was grown at 585°C in 0.25 mbar O_2 . In the case of epitaxial PTO films grown on $\text{SrRuO}_3/\text{SrTiO}_3(100)$, it was reported that the PTO films are in a monodomain state, with polarization oriented upwards.¹⁵ For $\text{PbZr}_{0.2}\text{Ti}_{0.8}\text{O}_3$ epitaxial films grown on $\text{SrTiO}_3(100)$ with a $\text{La}_{0.5}\text{Sr}_{0.5}\text{CoO}_3$ bottom electrode, it was reported that the ferroelectric film has an out-of-plane polarization preferentially oriented towards the bottom electrode.¹⁶ These observations reveal the importance of the electronic properties of the bottom electrode/ferroelectric film epitaxial interface and also of the details of the growth procedure, in the stabilization of a preferential orientation of the polarization of the ferroelectric epitaxial film.

Summarizing, we fabricated large range ordered arrays of $\text{La}_{0.7}\text{Sr}_{0.3}\text{MnO}_3$ and SrRuO_3 epitaxial dots and embedded the dots in ferroelectric PbTiO_3 epitaxial films. The PbTiO_3 film grown on top of the $\text{La}_{0.7}\text{Sr}_{0.3}\text{MnO}_3$ dots shows peculiar ordered 180° domains, which are switchable and have good ferroelectric properties, whereas the PbTiO_3 film made on top of SrRuO_3 dots has a uniform polarization state. Our observations allow us to propose a route of fabricating large arrays of switchable 180° ferroelectric domains.

We thank Norbert Schammelt for the fabrication of the FIB-TEM specimens and Dr. Eckhard Pippel for assistance with the Titan microscope. This work was partly supported by the German Science Foundation (DFG) within SFB762.

- ¹J. Ma, J. Hu, Z. Li, and C.-W. Nan, *Adv. Mater.* **23**, 1062 (2011).
- ²L. Yan, Y. Yang, Z. Wang, Z. Xing, J. Li, and D. Viehland, *J. Mater. Sci.* **44**, 5080 (2009).
- ³I. Vrejoiu, D. Hesse, M. Alexe, and U. Gösele, *Adv. Funct. Mater.* **18**, 3892 (2008).
- ⁴A. Morelli, F. Johann, N. Schammelt, and I. Vrejoiu, *Nanotechnology* **22**, 265303 (2011).
- ⁵A. Schilling, D. Byrne, G. Catalan, K. G. Webber, Y. A. Genenko, G. S. Wu, J. F. Scott, and J. M. Gregg, *Nano Lett.* **9**, 3359 (2009).
- ⁶E. J. Kim, J. L. R. Watts, B. Harteneck, A. Scholl, A. Young, A. Doran, and Y. Suzuki, *J. Appl. Phys.* **109**, 07D712 (2011).
- ⁷W. Lee, H. Han, A. Lotnyk, A. M. Schubert, S. Senz, M. Alexe, D. Hesse, S. G. Baik, and U. Gösele, *Nat. Nanotech.* **3**, 402 (2008).
- ⁸S. V. Kalinin, A. N. Morozovska, L. Q. Chen, and B. J. Rodriguez, *Rep. Prog. Phys.* **73**, 056502 (2010).
- ⁹C. V. Cojocaru, R. Nechache, C. Harnagea, A. Pignolet, and F. Rosei, *Appl. Surf. Sci.* **256**, 4777 (2010).
- ¹⁰P. M. te Riele, G. Rijnders, and D. H. A. Blank, *Appl. Phys. Lett.* **93**, 233109 (2008).
- ¹¹R. Hillebrand, E. Pippel, D. Hesse, and I. Vrejoiu, *Phys. Stat. Sol. A*, (submitted).
- ¹²M. Huijben, L. W. Martin, Y.-H. Chu, H. M. Holcomb, P. Yu, G. Rijnders, D. H. A. Blank, and R. Ramesh, *Phys. Rev. B* **78**, 094413 (2008).
- ¹³Y. J. Chang, C. H. Kim, S.-H. Phark, Y. S. Kim, J. Yu, and T. W. Noh, *Phys. Rev. Lett.* **103**, 057201 (2009).
- ¹⁴C.-L. Jia, K. Urban, M. Alexe, D. Hesse, and I. Vrejoiu, *Science* **331**, 1420 (2011).
- ¹⁵A. Morelli, S. Venkatesan, B. J. Kooi, G. Palasantzas, and J. Th. M. De Hosson, *J. Appl. Phys.* **105**, 064106 (2009).
- ¹⁶A. Roelofs, N. A. Pertsev, R. Waser, F. Schlaphof, L. M. Eng, C. Ganpule, V. Nagarajan, and R. Ramesh, *Appl. Phys. Lett.* **80**, 1424 (2002).